Interplay of anisotropies of momentum distribution and mean field in heavy-ion collisions

Christian H. Simon and Paweł Danielewicz

Phys. Rev. C **87**, 054619 — Published 28 May 2013

DOI: 10.1103/PhysRevC.87.054619

Interplay of anisotropies of momentum distribution and mean field in heavy-ion collisions

Christian H. Simon[1, 2, *] and Paweł Danielewicz[2, †]

[1] *Physikalisches Institut and Department of Physics and Astronomy, Ruprecht-Karls-Universität Heidelberg, D-69120 Heidelberg, Germany*

[2] *National Superconducting Cyclotron Laboratory and Department of Physics and Astronomy, Michigan State University, East Lansing, Michigan 48824, USA*

(Dated: May 1, 2013)

Abstract

Background: Two important parametrizations of momentum-dependent nucleonic fields, proposed for the simulations of central heavy-ion collisions, one by Gale *et al.* and the other by Welke *et al.*, suffer from practical limitations. The first gives rise to mean fields isotropic in momentum, even when underlying momentum distributions are anisotropic, making descriptions of early non-equilibrium stages of collisions unrealistic. The second parametrization gives rise to anisotropic mean fields, but is computationally expensive, since the mean field has to be computed separately for every location of a nucleon in phase-space, through folding.

Purpose: Here, we construct a parametrization of the nucleonic mean field, that yields an anisotropic mean field for an anisotropic momentum distribution and is inexpensive computationally. To demonstrate the versatility of our parametrization, we take the case of results from the parametrization by Welke *et al.* and attempt to approximate them.

Method: In arriving at a suitable anisotropic mean field potential, we draw, on one hand, from the idea behind the parametrization of Gale *et al.*, of a separable expansion of the potential energy, and, on the other, from the idea of a parallel expansion of the energy and mean field, in anisotropy.

Results: We show that using our novel parametrization we can qualitatively and partially quantitatively reproduce the features of the mean-field parametrization of Welke *et al.*.

Conclusions: This opens up the possibility of exploring the effects of mean-field anisotropy in collisions, without the penalty of computational cost behind the folding parametrization.

PACS numbers: 25.70.-z, 21.65.Mn

Keywords: nuclear matter, heavy-ion collisions, transport theory, momentum anisotropy

* csimon@physi.uni-heidelberg.de

† danielewicz@nscl.msu.edu

I. INTRODUCTION

Heavy-ion collisions are complex events on account of many physical effects competing in the dynamics. To effectively simulate the collisions, simplifying assumptions and approximations need to be adopted. Fortunately, excessive details are likely not essential for overall outcomes of those simulations, given superposition of the effects over space and reaction history and the fact that reaction observables tend to exhibit smooth variations with characteristics of the reactions and measurement criteria.

Complexity and effective averaging over space and history in the collisions make it tempting to simplify calculations at the level of numerical decisions. However, this type of simplifications have led to the commonplace for the collision simulations, where simulations with the same or similar physical assumptions yield[1] different predictions for observables [1]. Indeed, it is difficult to judge the quality of approximations, if an exact limit cannot be approached. With this, it can be beneficial to adopt simplifications at the level of the theory for the collisions, in such a fashion that, on one hand, any sought interesting physical effects can be captured and, on the other, the exact solution may be approached in a systematic manner. The limit of exact solution can then serve to validate the approximations, in addition to the conservation laws [2]. In this context, we address here the formulation of momentum dependence within the transport theory for heavy-ion collisions.

To provide the background, the heavy-ion collisions are commonly described in simulations in terms of phase-space Wigner distributions f, for nucleons and other particles, that follow the Boltzmann-Uehling-Uhlenbeck (BUU) [3] equation with nucleon optical potential U. An efficient way of solving the equation involves representing f in terms of test-particles [4], $N_{\rm t}$ per physical nucleon, with exact solution to the equations approached for $N_{\rm t} \to \infty$. The collisions offer, in particular, a unique opportunity of studying U at supranormal densities [5]. The interplay of the momentum dependence of the nucleon optical potential U and collision observables turned to be of utmost importance in the heavy-ion collision theory. Not only does momentum dependence play a significant role in generation of collective flow, according to the transport calculations [6], but it is also crucial for particle production [7]. In particular, in order to properly constrain the nuclear compression

[1] Community meetings have been dedicated to the issue, in particular at ECT* Trento in 2003 [1] and 2006.

modulus K, defined as

$$K = p_{\rm F}^2 \frac{d^2(E/A)}{dp_{\rm F}^2} \ , \tag{1}$$

where $p_{\rm F}$ is the Fermi momentum and E/A the binding energy per nucleon, one must take the momentum dependence of nucleon-nucleon interactions into account. In 1976, Blaizot *et al.* [8] showed that K could be inferred by measuring the energy of the isoscalar monopole resonance in medium and heavy nuclei, and arrived at the value of $K = 210 \pm 30\,\mathrm{MeV}$. Flow data, however, for quite some time seemed to be describable by both a momentum-dependent "soft" eos ($K \approx 210\,\mathrm{MeV}$) or a momentum-independent "hard" eos ($K \approx 380\,\mathrm{MeV}$) [9, 10]. Eventually, though, it became possible to decide on the momentum dependence with heavy-ion observables. Pan and Danielewicz [6] demonstrated that the best agreement between sideward flow data and the results from transport calculations could be obtained when applying a momentum-dependent "soft" eos.

Several approaches to the momentum dependence of the optical potential have been put forward in the literature (see [11] for a review article). The particularly well-known parametrizations, utilized directly or indirectly in BUU calculations, are the early parametrization by Gogny [12], the ansatz by Gale, Bertsch and Das Gupta [10] and the one by Welke *et al.* [13]. In Sec. II, the latter two parametrizations are discussed in more detail, and the results by Welke *et al.* serve as a reference for our calculations. Following Landau quasiparticle theory [14], inherent in these approaches are functional expressions for the potential energy density V and for its functional derivative with respect to the single-particle phase-space density $f(\mathbf{r}, \mathbf{p})$,

$$U = \left. \frac{\delta V}{\delta f} \right|_{\mathbf{p}} \ , \tag{2}$$

namely the nucleonic mean field (or optical potential) U.

The important aspect of the formulation of Gale *et al.* [10], of the momentum-dependent potential, is that the effort in integrating [2] the mean-field part of the BUU equation grows linearly with the test-particle number $N_{\rm t}$, paralleling the case of momentum-independent U, making it easy to approach the limit of an exact solution. On the other hand, the effort in integrating the equation with the potential from Welke *et al.* [13] grows as $N_{\rm t}^2$. The calculational convenience of [10] comes, though, at a price in that the optical potential U ends up being isotropic in momentum space. However, if the phase-space density f is anisotropic in momentum space, one may expect U to be anisotropic as well. The deficiency of the

formulation by Gale *et al.* [10] is likely to get more and more serious the higher the energy of the collision and especially at the early stages of the collision when f is most anisotropic. Here, we show that it is possible to extend the formulation [10] to arrive at U anisotropic in momentum, without scaling up the calculational effort as in [13]. To demonstrate the flexibility of the new formulation for U, we take on the formulation by Welke *et al.* and attempt to reproduce its results for f representing typical situations in heavy-ion collisions.

Our work is based on the M.Sc. Thesis [15]. In our strategy, for the sake of intrinsic consistency, we start out by considering the potential energy V of a system anisotropic in momentum and derive U from V (2). We parametrize V taking into account, on one hand, general physical expectations and, on the other, the need to carry out efficiently BUU transport calculations, such as within the code by Danielewicz [5], while ensuring the capability to explore different anisotropies of U. The construction of V involves introducing separable interactions in p-space where different terms can represent different spherical harmonics through which the anisotropy explicitly enters the mean field. We attempt to make our approach suitable for different stages of a heavy-ion collision. In comparing our results to those of Welke *et al.*, for partially equilibrated f, we describe the anisotropy of f in terms of an axial anisotropy parameter ε. In addressing the first stages of collisions, we consider the situation of two separated Fermi spheres in momentum space, for projectile and target. Several efforts in the literature [16–18], with the goal of coping with the early-stage momentum-anisotropies, specifically consider the latter type of superposition.

The work is organized as follows. In Sec. II, we present the models by Gale, Bertsch, Das Gupta (GBD) and by Welke *et al.* (WPKDG). The WPKDG model, requiring the determination of a 3-dimensional integral for every relevant phase-space location, at every time step of a BUU calculation, is computationally very costly. By contrast, GBD requires the determination of integrals only for every relevant spatial location. In that section we also introduce our own ansatz for V and U, based on a spherical harmonics expansion (SHE). That ansatz also requires the determination of integrals only for every relevant spatial location. Our SHE results for ground-state, excited-state and collision scenarios are represented in Sec. III, and our approach is tested there against the WPKDG parametrization. The benefits of SHE for BUU calculations, in terms of increased computational efficiency and reduced Monte-Carlo noise, which are disadvantages of WPKDG, are outlined in Sec. IV.

II. THEORETICAL CONSIDERATIONS

A. Implicit anisotropy in mean fields

The special feature of GBD is that it is formulated in the local frame where the average nucleonic momentum $\langle \mathbf{p} \rangle$ vanishes. Alternatively, the nucleonic momenta may be specified relative to $\langle \mathbf{p} \rangle$ in another frame. This may be contrasted with WPKDG. Both models are based on Skyrme-type interactions [19] for the density-dependent part of the energy density and the mean field. In the case of GBD, the potential energy density can be written as [10]

$$\begin{aligned} V_{\mathrm{GBD}}(\rho(\mathbf{r})) = & \frac{A}{2}\frac{\rho^2(\mathbf{r})}{\rho_0} + \frac{B}{\sigma+1}\frac{\rho^{\sigma+1}(\mathbf{r})}{\rho_0^\sigma} \\ & + C\,\frac{\rho(\mathbf{r})}{\rho_0}\int d^3p'\,\frac{f(\mathbf{r},\mathbf{p}')}{1+\left[\frac{\mathbf{p}'-\langle\mathbf{p}\rangle}{\Lambda}\right]^2}\,. \end{aligned} \tag{3}$$

Accordingly, following (2), one obtains the nucleonic mean field

$$\begin{aligned} U_{\mathrm{GBD}}(\rho(\mathbf{r}),\mathbf{p}) = & A\left(\frac{\rho(\mathbf{r})}{\rho_0}\right) + B\left(\frac{\rho(\mathbf{r})}{\rho_0}\right)^\sigma \\ & + \frac{C}{\rho_0}\int d^3p'\,\frac{f(\mathbf{r},\mathbf{p}')}{1+\left[\frac{\mathbf{p}'-\langle\mathbf{p}\rangle}{\Lambda}\right]^2} \\ & + \frac{C}{\rho_0}\frac{\rho(\mathbf{r})}{1+\left[\frac{\mathbf{p}-\langle\mathbf{p}\rangle}{\Lambda}\right]^2}\,. \end{aligned} \tag{4}$$

Note that f – where not otherwise stated – represents the single-particle phase-space density, normalized according to $\rho(\mathbf{r}) = \int d^3p'\, f(\mathbf{r},\mathbf{p}')$.

Within WPKDG, the energy density is parametrized as [13]

$$\begin{aligned} V_{\mathrm{WPKDG}}(\rho(\mathbf{r})) = & \frac{A}{2}\frac{\rho^2(\mathbf{r})}{\rho_0} + \frac{B}{\sigma+1}\frac{\rho^{\sigma+1}(\mathbf{r})}{\rho_0^\sigma} \\ & + \frac{C}{\rho_0}\int\int d^3p\, d^3p'\,\frac{f(\mathbf{r},\mathbf{p})f(\mathbf{r},\mathbf{p}')}{1+\left[\frac{\mathbf{p}-\mathbf{p}'}{\Lambda}\right]^2}\,. \end{aligned} \tag{5}$$

This leads to the mean field of the form

$$\begin{aligned} U_{\mathrm{WPKDG}}(\rho(\mathbf{r}),\mathbf{p}) = & A\left(\frac{\rho(\mathbf{r})}{\rho_0}\right) + B\left(\frac{\rho(\mathbf{r})}{\rho_0}\right)^\sigma \\ & + 2\frac{C}{\rho_0}\int d^3p'\,\frac{f(\mathbf{r},\mathbf{p}')}{1+\left[\frac{\mathbf{p}-\mathbf{p}'}{\Lambda}\right]^2}\,. \end{aligned} \tag{6}$$

Inherent in both models are the 5 parameters A, B, σ, C and Λ. From those parameters, σ is particularly strongly tied to the incompressibility K, while Λ determines the high-p behavior

of U. To constrain the parameters, a demand is placed that the energy per nucleon minimizes with $E/A = -16\,\mathrm{MeV}$ at the saturation density $\rho_0 = 0.16\,\mathrm{fm}^{-3}$. For both parametrizations, GBD and WPKDG, the incompressibility is chosen equal to $K \simeq 215\,\mathrm{MeV}$, and the effective mass ratio at saturation momentum is $m^*/m \simeq 0.7$. For WPKDG, specific values of the potential at ρ_0 are $U(\rho_0, p = 0) \simeq -75\,\mathrm{MeV}$ and $U(\rho_0, p^2/2m \simeq 300\,\mathrm{MeV}) = 0$. The GBD parametrization may be considered an approximation to WPKDG, and this issue has been explored to a degree in [13]. With SHE we want to develop a qualitatively better approximation to WPKDG, while still keeping the method computationally inexpensive, as GBD.

B. Explicit anisotropy in mean fields

The essential idea of SHE, borrowed from GBD [10], is that of a separable representation for the energy functional. A separable representation, with a limited number of terms, could be adjusted to represent results from microscopic theory, obtained for different non-equilibrium situations, such as Dirac-Brueckner [20]. In lieu of a microscopic theory, we take the intuitively appealing WPKDG parametrization and examine to what extent we can reproduce its results with SHE. If we can be successful here, we may be successful with a microscopic theory as well. Otherwise, following a phenomenological strategy, as common in heavy-ion collisions, we may use SHE as the starting point and see whether collision observables can constrain the energy functional constructed within SHE. Besides the separable part of the energy, generating momentum dependence of U, we employ a ρ-dependent part of the Skyrme form, such as in GBD or WPKDG. When aiming at a minimal number of terms in the separable expansion, while retaining the capability of describing mean fields anisotropic in momentum, our energy functional in SHE consists of Skyrme and separable scalar and tensorial quadrupole terms:

$$\begin{aligned} V_{\mathrm{SHE}}(\rho(\mathbf{r})) = \quad & \frac{A}{2}\frac{\rho^2(\mathbf{r})}{\rho_0} + \frac{B}{\sigma+1}\frac{\rho^{\sigma+1}(\mathbf{r})}{\rho_0^{\sigma}} \\ & + \frac{C}{\rho_0}\left[\left(\int d^3p' \, \frac{f(\mathbf{r},\mathbf{p}')}{1+\left[\frac{\mathbf{p}'}{\Lambda_{\mathrm{iso}}}\right]^2}\right)^2 \right. \\ & \left. + \sum_{\alpha,\beta} T^{\alpha\beta}(\mathbf{r})\, T^{\alpha\beta}(\mathbf{r})\right]. \end{aligned} \tag{7}$$

We do not include a dipole separable term, which we expect to be small in the center of mass. A dipole term is accounted for in the relativistic approach of Reference [21]. To demonstrate the robustness of such a representation we will attempt to show that the results from the folding model WPKDG can be well approximated within our separable model, including the reproduction of anisotropies of U. For simplicity, we take both the scalar and the tensor term as symmetric in two single-particle quantities, presuming dominance of 2-body interactions. Inclusion of a tensor term makes our parametrization different from GBD, scalar in our terminology. However, we take the form of the single-particle factor to be the same as in GBD [10]. In the above, $T^{\alpha\beta}$ is a second-rank Cartesian tensor [22, 23]:

$$T^{\alpha\beta}(\mathbf{r}) \equiv \int d^3p'\, c(p')\, f(\mathbf{r},\mathbf{p}')\, (p'^{\alpha}p'^{\beta} - \frac{1}{3}\, p'^2\delta^{\alpha\beta})\ . \tag{8}$$

An important feature is its tracelessness,

$$T^{xx} + T^{yy} + T^{zz} = 0\ . \tag{9}$$

For the functional form of $c(p)$ in (8) we choose

$$c(p) = \frac{1}{p^2 + \Lambda_{\text{aniso}}^2}\ . \tag{10}$$

Note the parameters Λ_{iso} in the scalar part of (7) and Λ_{aniso} in the tensorial part, which we introduced in addition to the ones inherited from GBD and WPKDG.

According to (2), the optical potential is found by taking the functional derivative of (7) with respect to f. Due to the directionality involved and approximate axial symmetry of the phase-space density in heavy-ion collisions, the off-diagonal elements of (8) are negligible in practice, reducing the summation over α, β to diagonal elements only. Here the tracelessness (9) of the tensor comes into play, allowing us to express all elements in terms of T^{zz} when dependence on transverse direction is weak. Upon taking a functional derivative of (7) and transforming to spherical coordinates we get

$$\begin{aligned} U_{\text{SHE}}(\rho(\mathbf{r}),\mathbf{p}) = \quad & A\left(\frac{\rho(\mathbf{r})}{\rho_0}\right) + B\left(\frac{\rho(\mathbf{r})}{\rho_0}\right)^{\sigma} \\ & + \frac{C}{\rho_0}\Bigg[\frac{2}{1+\left[\frac{\mathbf{p}}{\Lambda_{\text{iso}}}\right]^2}\int d^3p'\,\frac{f(\mathbf{r},\mathbf{p}')}{1+\left[\frac{\mathbf{p}'}{\Lambda_{\text{iso}}}\right]^2} \\ & + \sqrt{\frac{16\pi}{5}}\, c(p)\, p^2\, Y_{20}(\vartheta)\, T^{zz}(\mathbf{r})\Bigg]. \end{aligned} \tag{11}$$

Here we used the definition of the spherical harmonic of degree 2 and order 0,

$$Y_{20}(\vartheta) = \sqrt{\frac{5}{16\pi}}\left(3\cos^2(\vartheta) - 1\right). \tag{12}$$

Therewith, the SHE optical potential (11) depends on anisotropy explicitly. The decisive last term vanishes for isotropic f since T^{zz} is zero for such cases by construction.

III. RESULTS

A. Ground-state properties

As in GBD and WPKDG, we demand that E/A for SHE minimizes at $\rho_0 = 0.16\,\mathrm{fm}^{-3}$ with the value of $E/A = -16\,\mathrm{MeV}$. For consistency with the other parametrizations, we further demand that $K \simeq 215\,\mathrm{MeV}$, and $m^*/m \simeq 0.7$ at the Fermi momentum of $p_\mathrm{F}^{(0)} = 263\,\mathrm{MeV/c}$ at ρ_0. Otherwise, it would be natural to require that SHE reproduced the momentum dependence of WPKDG for the ground-state phase-space density

$$f(\mathbf{r},\mathbf{p}) = \frac{g}{(2\pi\hbar)^3}\,\theta(p_\mathrm{F}^{(0)} - |\mathbf{p}|)\,, \tag{13}$$

where the degeneracy factor is $g = 4$. In fact, by adjusting the parameters of SHE the momentum dependencies at ρ_0 can be made nearly indistinguishable. However, then differences between SHE and WPKDG may be excessive in some non-equilibrium situations. Correspondingly we adopt a compromise choosing parameters so that the results have a similar appearance under different circumstances, but can exhibit quantitative discrepancies.

At zero temperature, calculations of energy and optical potential can be largely done analytically. A couple of integrals useful for the purpose are provided in the Appendix. With spatial density of kinetic energy given by

$$\left\langle \frac{p^2}{2m} \right\rangle = \int d^3p' \frac{p'^2}{2m} f(\mathbf{r},\mathbf{p}')\,, \tag{14}$$

the energy per nucleon is

$$E/A = \int d^3r \left[\left\langle \frac{p^2}{2m} \right\rangle + V[f] \right] /A\,. \tag{15}$$

From the energy, the incompressibility K is calculated and, from U, the effective mass ratio is determined,

$$\frac{m^*}{m} = \frac{p}{m}\left(\frac{d}{dp}\left[\frac{p^2}{2m} + U(\rho(\mathbf{r}),\mathbf{p}) \right] \right)^{-1}. \tag{16}$$

The parameters for SHE, as well as GBD and WPKDG are provided in Table I. Figure 1 shows the potential energy density for the three interaction parametrizations and Fig. 2 displays the energy per nucleon. Next, Fig. 3 shows the incompressibility as a function of density ρ and Fig. 4 shows the effective mass ratio at ρ_0, as a function of momentum. Finally, Fig. 5 shows the optical potential as a function of momentum at the normal density. As we stated, by adjusting the parameters in SHE, we could obtain an excellent agreement between SHE and WPKDG in Figs. 4 and 5, but that at the cost of poorer agreement in other situations.

B. Excited nuclear matter

To study suitability of SHE for describing situations in excited but not fully equilibrated matter, we consider results from SHE and WPKDG for a phase-space density which has the form of an anisotropic Gaussian in momentum:

$$f(\mathbf{r},\mathbf{p}) = \frac{\rho(\mathbf{r})}{(2\pi\sigma_{\rm g}^2)^{3/2}} \exp\left[-\frac{1}{2\sigma_{\rm g}^2}\left(p_\perp^2(1+\varepsilon) + \frac{p_\parallel^2}{(1+\varepsilon)^2}\right)\right] . \tag{17}$$

Here, ε is a parameter that regulates anisotropy of the momentum distribution that is axially symmetric about the longitudinal axis. Changes in ε simultaneously change the longitudinal and transverse widths in such a manner that the density ρ associated with f does not change. Physically allowed values are $\varepsilon > -1$ and increasing ε makes the distribution more prolate. One needs to relate the parameters ε and $\sigma_{\rm g}$ to other, e.g. such as temperature, in order to determine interesting parameter ranges. We refer to the kinetic energy density (14) to advance in our considerations. While an isotropic Gaussian ($\varepsilon = 0$) yields the density

$$\left\langle \frac{p^2}{2m} \right\rangle = 3\frac{\sigma_{\rm g}^2}{2m}\rho \, , \tag{18}$$

for an anisotropic Gaussian ($\varepsilon \neq 0$) one obtains

$$\left\langle \frac{p^2}{2m} \right\rangle = \frac{\sigma_{\rm g}^2}{2m}\left[\frac{2}{(1+\varepsilon)} + (1+\varepsilon)^2\right]\rho \, . \tag{19}$$

Recalling the Boltzmann model, Gaussian standard deviation σ (for one direction) and temperature T are connected via

$$\sigma^2 = m_{\rm N} T \, , \tag{20}$$

where m_{N} is the nucleon mass. Effective temperatures between $15\,\mathrm{MeV} \leq T \leq 170\,\mathrm{MeV}$ are of interest in heavy-ion collisions. We assume that, on approach to equilibrium, the distributions are not more narrow than representing $T = 15\,\mathrm{MeV}$ and not much more spread out than representing $T = 170\,\mathrm{MeV}$. With this, we arrive at the anisotropy range $-0.6 \lesssim \varepsilon \lesssim 1.5$. In the results that follow for $\rho = 2\rho_0$, we use the relatively low $\sigma_{\mathrm{g}} = 150\,\mathrm{MeV/c}$, which allows for relatively strong momentum dependencies in U, at low momenta. The subsequent Figs. 6–10 show the obtained values of optical potential both in the SHE and WPKDG parametrizations, at different momenta p (in multiples of ground-state $p_{\mathrm{F}}^{(0)}$, Sec. III A) in $\rho = 2\rho_0$ matter with different momentum anisotropies, as a function of angle relative to the symmetry axis of the distribution. In the figures, we can see rather good correspondence between the results for the two parametrizations. While the SHE parametrization explicitly follows the shape of Y_{20}, it is approximately also the case for WPKDG. Apparently higher multipolarity terms in a separable expansion for WPKDG are negligible. This is likely helped by the smoothness of the momentum distribution. Notably in heavy-ion collisions the momentum distributions tend to evolve to a smooth form rather quickly, making the close correspondence between the results likely in practice.

C. Idealized collision scenario

The final test situation that we consider, potentially the most challenging for a description such as SHE, is the early stage of a heavy-ion collision, where interpenetration of the opposing nuclei has started but no equilibration has yet occurred. To represent such a situation, Welke *et al.* took a momentum distribution with two Fermi spheres, each representing the ground-state of saturated matter

$$f(\mathbf{r},\mathbf{p}) = \frac{g}{(2\pi\hbar)^3}\,\theta(p_{\mathrm{F}}^{(0)} - |\mathbf{p} \mp \mathbf{p}_0/2|)\ , \tag{21}$$

separated by $p_0 = 800\,\mathrm{MeV/c}$ in momentum space. The scenario is sketched in Fig. 11. To account for relativistic effects in this colliding nuclear matter scenario, one would rather consider Fermi ellipsoids than spheres [16–18]. Such a Lorentz covariant treatment goes beyond the goals of the present paper. The optical potentials U (cf. Fig. 12) associated with it are plotted as functions of the polar angle ϑ (defined in Fig. 11) for different momenta. The vector momenta $\mathbf{p}$ are taken with reference to the center of one sphere, with the angle

relative to the symmetry axis of the system. The mean fields vary not only in overall offset, but also in dependence on angle. As a point of view additional to that in Welke *et al.* [13], presented above, we further consider the mean-field potential at different $\mathbf{p}$ relative to the c.m., as a function of angle ϑ about the c.m. (defined in Fig. 13). The SHE, WPKDG and GBD potentials are compared in this fashion in Fig. 14. Significant deviations can be seen between the potentials at lower momenta p, but lesser at the highest momentum towards the region where the nucleons are. By construction, the GBD potential is isotropic in this representation. The discrepancies at low momenta in Fig. 14 show limitations of the SHE approach. While we chose another phenomenological approach as reference here, rather than a microscopic theory for which sparse non-equilibrium results exist, we expect a difficulty for SHE, with just a couple of separable terms, to be universal when momentum distributions change abruptly with momentum. Fortunately, in heavy-ion collisions the distributions quickly evolve to a smooth form.

IV. DISCUSSION AND CONCLUSIONS

A. Application to transport simulations

Beyond the scope of this article is the actual application of the anisotropic mean field parametrization to reaction simulations, namely BUU calculations. However, in order to stress the practical relevance of our work, we will provide a brief prescription how to employ our results in reactions and name the benefits one should gain then.

The foundation of BUU methodology is the Boltzmann transport equation [4, 5] for the single-particle distribution function $f(\mathbf{p}, \mathbf{r}, t)$. In order to determine the state of the system one needs to solve the BUU equation for f in every time step t:

$$\frac{\partial f}{\partial t} + \frac{\partial \epsilon}{\partial \mathbf{p}} \frac{\partial f}{\partial \mathbf{r}} - \frac{\partial \epsilon}{\partial \mathbf{r}} \frac{\partial f}{\partial \mathbf{p}} = I_{\mathrm{coll}}(f) \; . \tag{22}$$

The collision integral on the r.h.s. of (22) accounts for the time evolution of the single-particle phase-space density f evoked by two-body collisions. The mean field U enters the Boltzmann equation on the l.h.s. which takes the motion of particles in the field into account. In order to find the single-particle energies ϵ one has to take the functional derivative of the

system's net energy E with respect to the phase-space density f:

$$\epsilon = \frac{\delta E}{\delta f} = \frac{p^2}{2m} + \frac{\delta V}{\delta f} = \frac{p^2}{2m} + U \ . \tag{23}$$

If the p-dependent part of the mean field is parametrized in terms of an integral

$$U(\mathbf{r}, \mathbf{p}) \propto \int d^3p' \, \frac{f(\mathbf{r}, \mathbf{p}')}{1 + \left[\frac{\mathbf{p}-\mathbf{p}'}{\Lambda}\right]^2} \ , \tag{24}$$

as in the model by Welke *et al.*, one has to determine a different 3-dimensional integral for every momentum $\mathbf{p}$ and position $\mathbf{r}$. When f is represented in terms of test-particles [4], N_t per nucleon, the integration is replaced by summation over the test-particles. With the need to calculate an integral at the phase-space position of every test-particle, the overall effort in calculating the mean field scales as N_t^2, forcing compromises at large N_t countering this rapid growth. On the other hand, in the framework of our SHE model, one would have to evaluate the integrals in the isotropic term and in T^{zz} once per time step for a given spatial location. With this, the effort in calculating the mean field would scale as N_t, just as for the GBD parametrization or p-independent U. The calculational effort reduced by a factor of the order of N_t, for the same accuracy, represents a significant advantage of our model over the WPKDG parametrization.

B. Summary

We developed a parametrization for the nucleonic mean field U, which explicitly exhibits an anisotropic behavior for anisotropic phase-space densities f, and that can significantly reduce computational effort and statistical noise in transport simulations, compared to current practice. On that account, we made the nuclear energy functional separable in momentum space, with different terms corresponding to different multipolarity in spherical angle. As reference and guideline during the process of setting up our model, the parametrization by Welke *et al.* [13] was used. We step by step evolved the elements of our model by breaking up the original – and in comparison to our parametrization very costly – convolution within the potential energy density, substituting it with separable scalar and tensorial terms, both symmetric in the single-particle properties, and by taking the functional derivative of V with respect to f to obtain U in a simple form. In addition to the Skyrme-type parameters in the ρ-dependent part, our model comprises two exclusive parameters, one of them – Λ_iso –

mainly relevant in isotropic scenarios, the other one – $\Lambda_{\rm aniso}$ – important for characterizing the anisotropy of the mean field. The latter phenomenological parameters represent range and are physically expected to be similar. In the framework of our SHE model we can reasonably well describe cold nuclear matter properties, obtain excellent results for equilibrated scenarios and find a good practical agreement for early stages of a colliding system. The latter situation has been dealt with in the literature [13]. We showed that our ansatz is generally applicable even when momentum population for the system changes abruptly.

To conclude, we presented a simple way of describing the potential energy density V and associated anisotropic momentum dependent mean field U in heavy-ion collisions. Flexibility in coping with interactions for anisotropic momentum distributions is important since local momentum anisotropies persist until late in the dynamics of heavy-ion collisions. Exploration of consequences of the anisotropies, however, should not be stacked against inabilities to carry out collision calculations, poor statistics or noise in the calculations. With the proposed approach, we believe, we resolve these issues.

ACKNOWLEDGMENTS

The authors would like to thank Brent W. Barker and Jun Hong for discussions. In particular we would like to express our gratitude to U. Mosel and T. Gaitanos for helpful comments and inspiring suggestions. This work was supported by National Science Foundation Grant Nos. PHY-0800026 and PHY-1068571.

Appendix: Analytical expressions for ground-state quantities

When dealing with Fermi spheres in cold matter scenarios one can find analytical results for the integrals over a Yukawa interaction kernel, appearing in (5), (6) and (11), for instance. Thus, one can circumvent many-dimensional numerical integrations. This obviously does not help in carrying out collision simulations, as the distributions quickly depart from the Fermi spheres. Particularly useful are the following identities:

$$\int_0^{p_{\rm F}}\int_0^{p_{\rm F}} d^3p\, d^3p' \frac{1}{1+\left[\frac{\mathbf{p}-\mathbf{p}'}{\Lambda}\right]^2} = \frac{32\pi^2}{3}p_{\rm F}^4\Lambda^2\Bigg[\quad \frac{3}{8} - \frac{\Lambda}{2p_{\rm F}}\arctan\frac{2p_{\rm F}}{\Lambda} - \frac{\Lambda^2}{16p_{\rm F}^2} + \left(\frac{3}{16}\frac{\Lambda^2}{p_{\rm F}^2} + \frac{1}{64}\frac{\Lambda^4}{p_{\rm F}^4}\right)\ln\left(1+\frac{4p_{\rm F}^2}{\Lambda^2}\right)\Bigg], \quad \text{(A.1)}$$

$$\int_0^{p_{\rm F}} d^3p' \frac{1}{1+\left[\frac{\mathbf{p}-\mathbf{p}'}{\Lambda}\right]^2} = \pi\Lambda^3\Bigg[\quad \frac{p_{\rm F}^2+\Lambda^2-p^2}{2p\Lambda}\ln\frac{(p+p_{\rm F})^2+\Lambda^2}{(p-p_{\rm F})^2+\Lambda^2} + \frac{2p_{\rm F}}{\Lambda} - 2\left(\arctan\frac{p+p_{\rm F}}{\Lambda} - \arctan\frac{p-p_{\rm F}}{\Lambda}\right)\Bigg]. \quad \text{(A.2)}$$

[1] E. E. Kolomeitsev *et al.*, J. Phys. G **31**, S741 (2005).

[2] R. J. Lenk and V. R. Pandharipande, Phys. Rev. C **39**, 2242 (1989).

[3] E. A. Uehling and G. E. Uhlenbeck, Phys. Rev. **43**, 552 (1933).

[4] G. F. Bertsch, H. Kruse, and S. Das Gupta, Phys. Rev. C **29**, 673 (1984).

[5] P. Danielewicz, Nucl. Phys. **A673**, 375 (2000).

[6] Q. Pan and P. Danielewicz, Phys. Rev. Lett. **70**, 2062 (1993).

[7] Q. Li, Z. Li, S. Soff, M. Bleicher, and H. Stöcker, J. Phys. G **32**, 151 (2006).

[8] J. P. Blaizot, D. Gogny, and B. Grammaticos, Nucl. Phys. **A265**, 315 (1976).

[9] J. Aichelin, A. Rosenhauer, G. Peilert, H. Stoecker, and W. Greiner, Phys. Rev. Lett. **58**, 1926 (1987).

[10] C. Gale, G. Bertsch, and S. Das Gupta, Phys. Rev. C **35**, 1666 (1987).

[11] J. Zhang, S. Das Gupta, and C. Gale, Phys. Rev. C **50**, 1617 (1994).

[12] D. Gogny, in *Nuclear Self Consistent Fields*, edited by G. Ripka and M. Porneuf (North-Holland, Amsterdam, 1975) p. 333.

[13] G. M. Welke, M. Prakash, T. T. S. Kuo, S. Das Gupta, and C. Gale, Phys. Rev. C **38**, 2101 (1988).

[14] P. Nozières and D. Pines, *The Theory Of Quantum Liquids*, Advanced Book Classics (Westview Press, Boulder, Colorado, 1999).

[15] C. H. Simon, *Interplay of Anisotropy of Momentum Distributions and Mean Fields in Heavy-Ion Collisions*, Master's Thesis, Michigan State University, East Lansing, Michigan (2011).

[16] T. Gaitanos, C. Fuchs, and H. H. Wolter, Nucl. Phys. **A650**, 97 (1999).

[17] C. Fuchs and T. Gaitanos, Nucl. Phys. **A714**, 643 (2003).

[18] T. Gaitanos, C. Fuchs, and H. H. Wolter, Nucl. Phys. **A741**, 287 (2004).

[19] T. H. R. Skyrme, Nucl. Phys. **9**, 615 (1959).

[20] C. Fuchs, L. Sehn, and H. H. Wolter, Prog. Part. Nucl. Phys. **30**, 247 (1993).

[21] T. Maruyama, W. Cassing, U. Mosel, S. Teis, and K. Weber, Nucl. Phys. **A573**, 653 (1994).

[22] J. Applequist, J. Phys. A **22**, 4303 (1989).

[23] P. Danielewicz and S. Pratt, Phys. Lett. **B618**, 60 (2005).

FIGURES

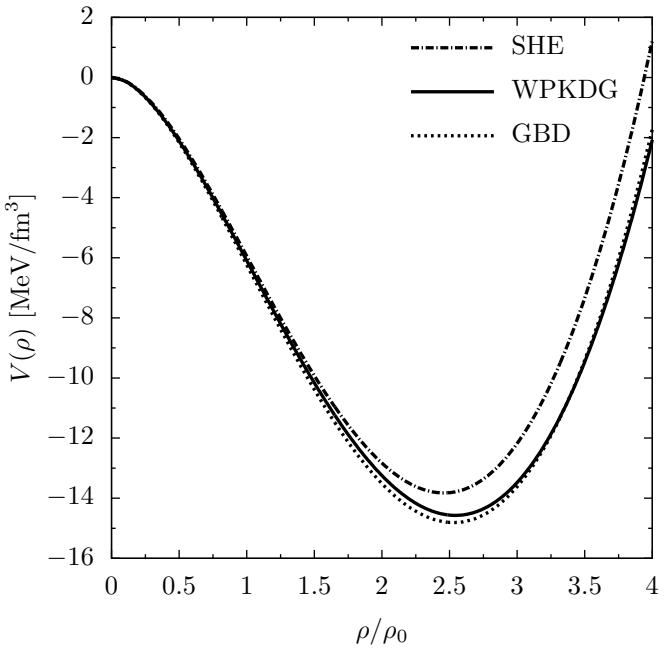

FIG. 1. Ground-state potential energy density as function of density of matter.

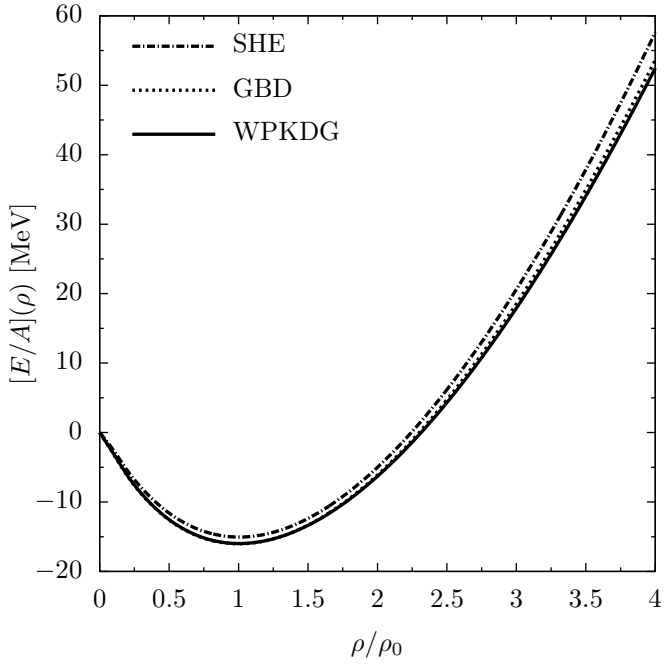

FIG. 2. Ground-state energy per nucleon as function of density of matter.

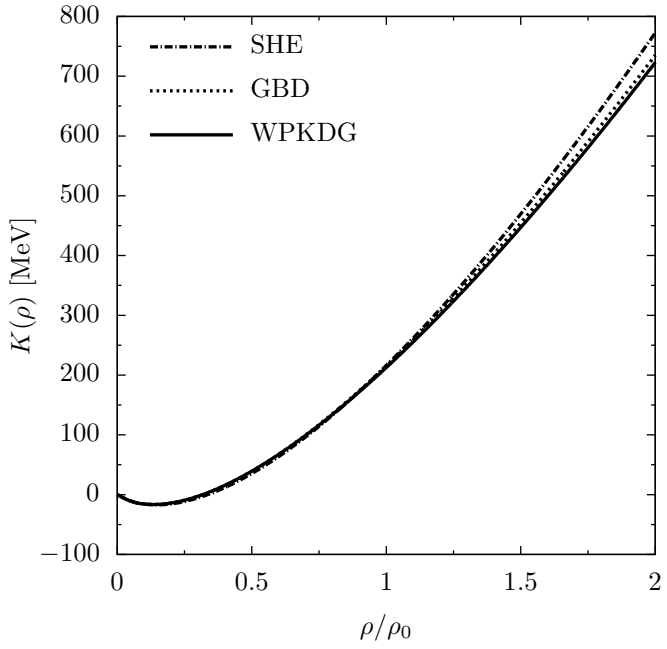

FIG. 3. Ground-state compressibility as function of density of matter.

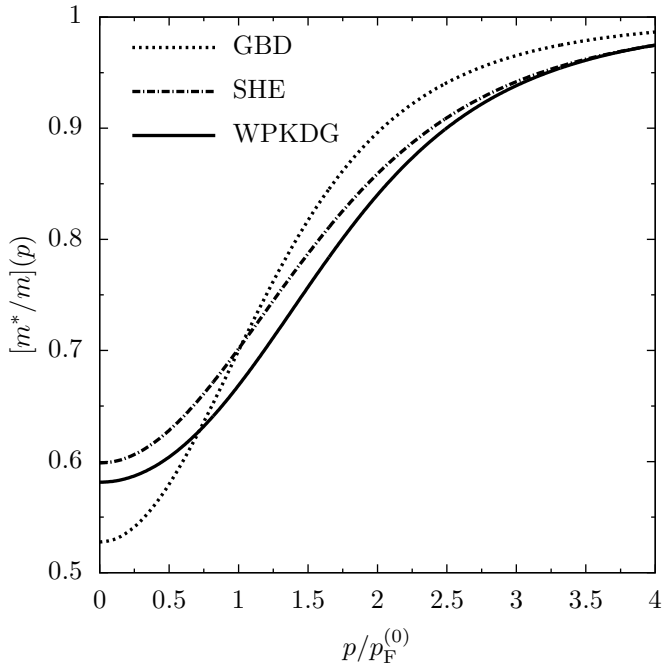

FIG. 4. Ground-state effective mass ratio as function of momentum, at normal density ρ_0.

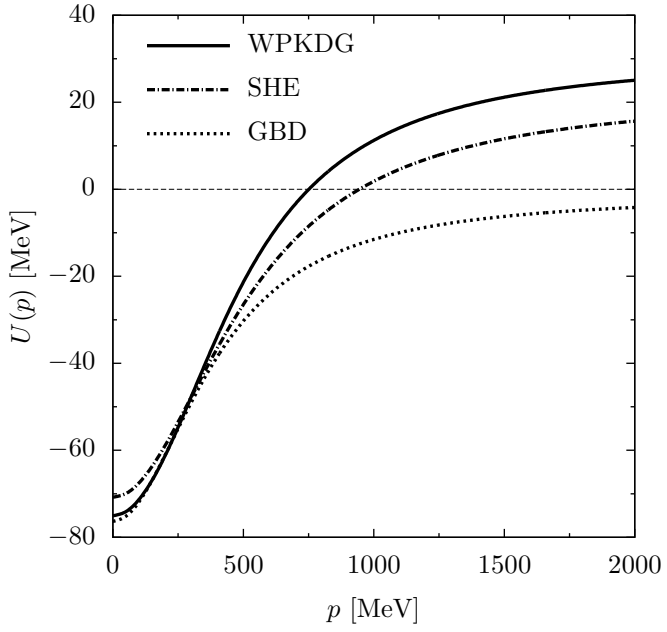

FIG. 5. Ground-state optical potential as function of momentum, at normal density ρ_0.

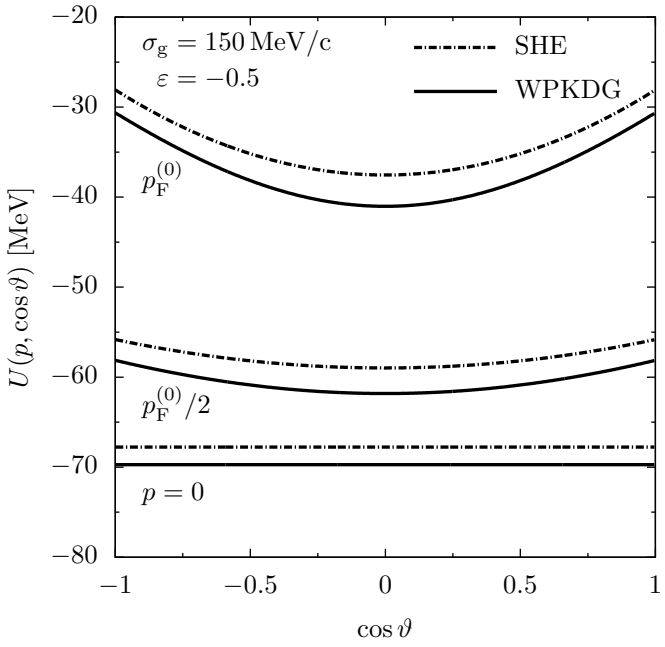

FIG. 6. Optical potential for an anisotropic momentum distribution (17) with $\varepsilon = -0.5$ at $\rho = 2\rho_0$, in the local c.m., for different indicated momenta p.

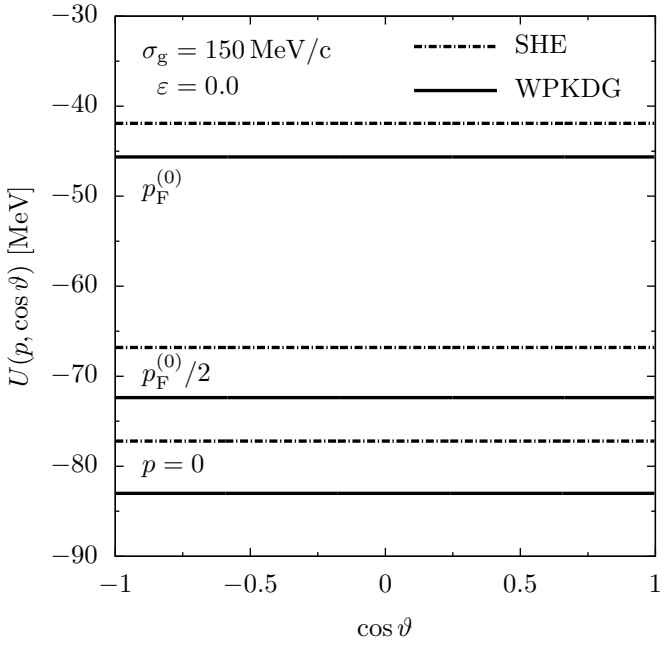

FIG. 7. Optical potential for an isotropic momentum distribution at $\rho = 2\rho_0$, in the local c.m., for different indicated momenta p.

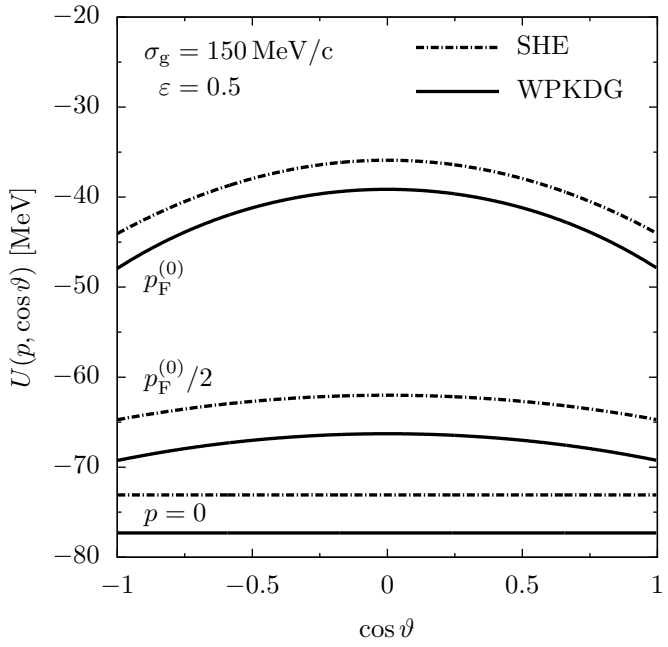

FIG. 8. Optical potential for an anisotropic momentum distribution with $\varepsilon = 0.5$ at $\rho = 2\rho_0$, in the local c.m., for different indicated momenta p.

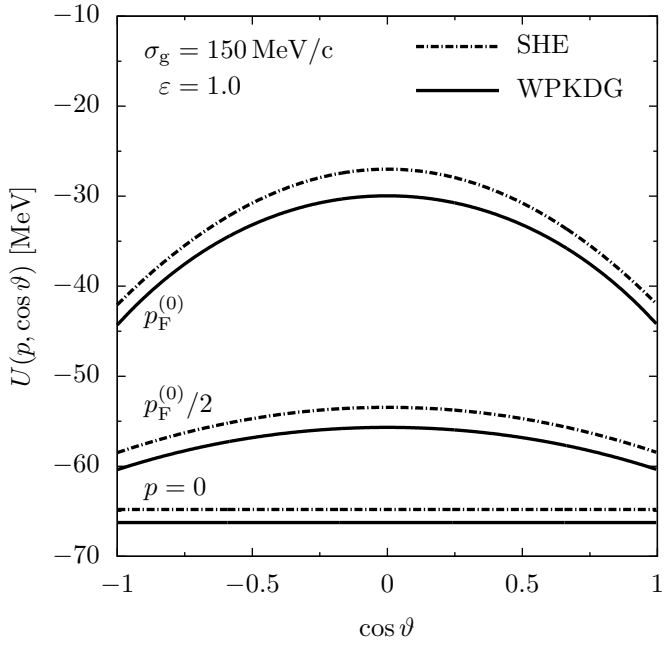

FIG. 9. Optical potential for an anisotropic momentum distribution with $\varepsilon = 1.0$ at $\rho = 2\rho_0$, in the local c.m., for different indicated momenta p.

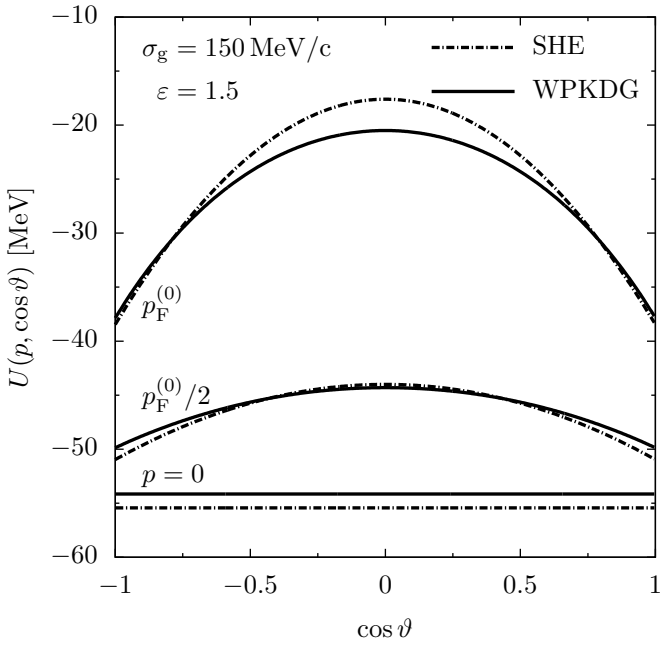

FIG. 10. Optical potential for an anisotropic momentum distribution with $\varepsilon = 1.5$ at $\rho = 2\rho_0$, in the local c.m., for different indicated momenta p.

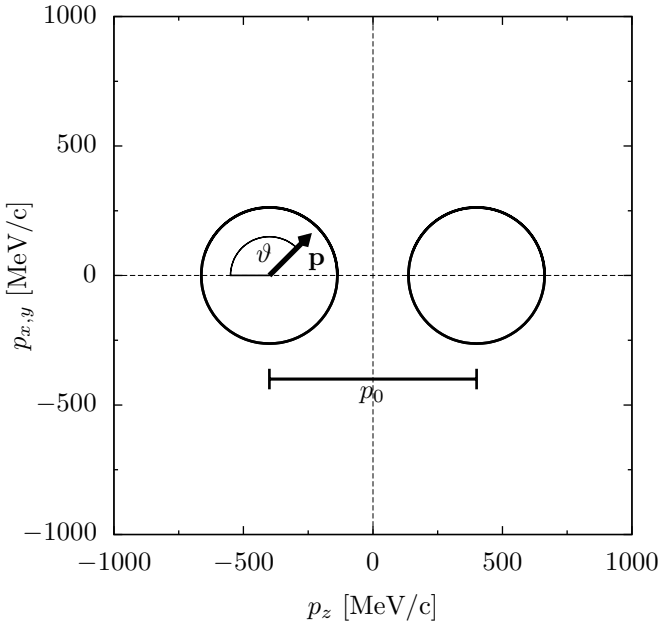

FIG. 11. Situation within the local rest frame of two Fermi spheres separated by p_0 in momentum space. The center of the left sphere serves as point of origin in the first examination of U for that situation.

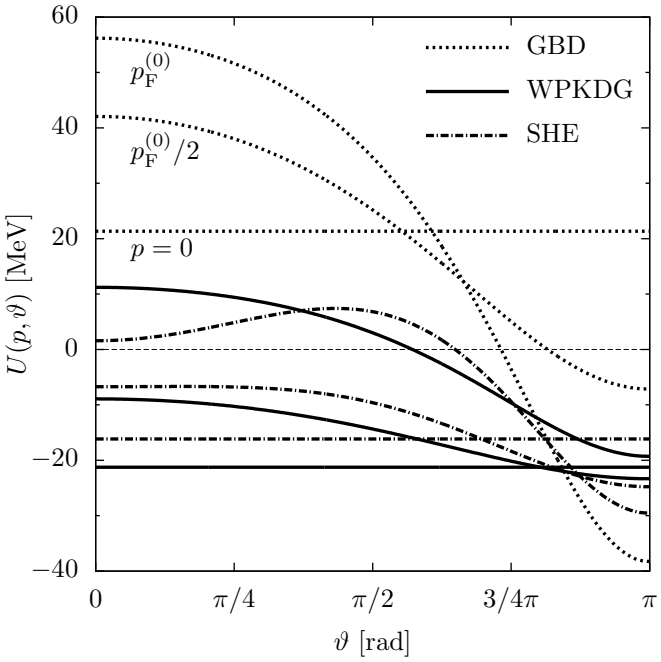

FIG. 12. Optical potential for the situation represented in Fig. 11, for different momenta relative to the center of one of the Fermi spheres, as a function of angle about that center, for the different parametrizations of the potential.

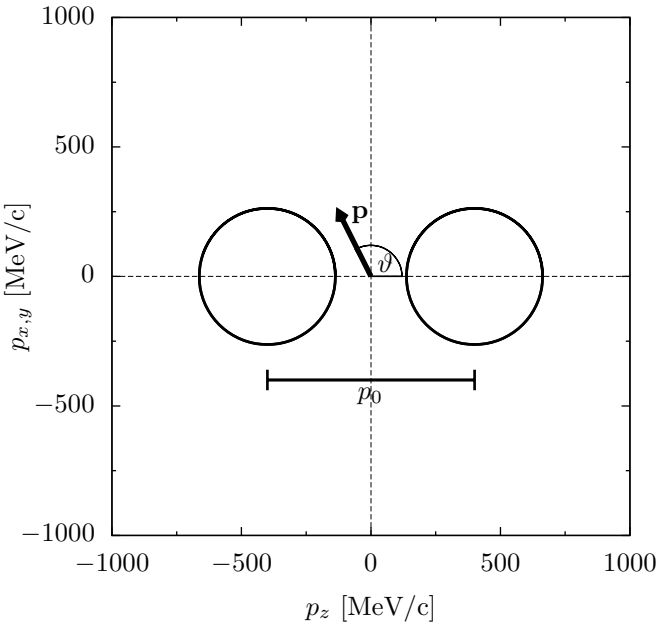

FIG. 13. Situation within the local rest frame of two Fermi spheres separated by p_0 in momentum space. The center of mass serves as point of origin in the second examination of U for that situation.

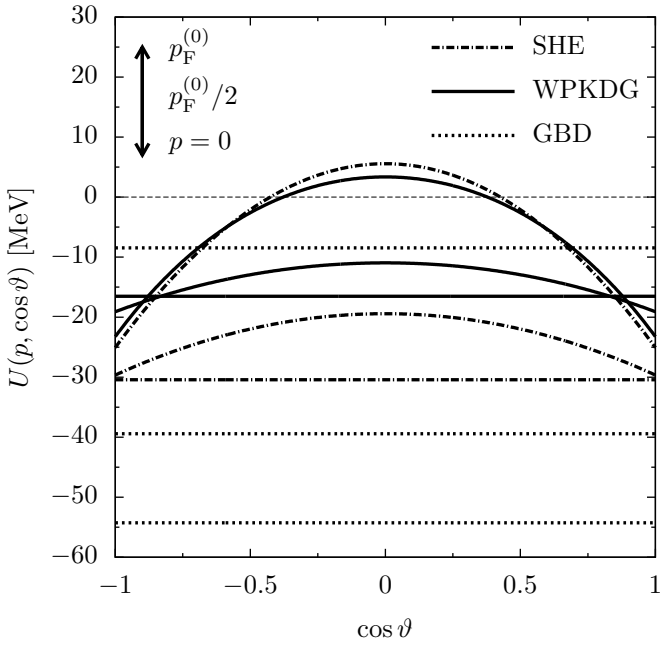

FIG. 14. Optical potential for the situation represented in Fig. 13, for different momenta relative to the local center of mass, as a function of angle about the center, for the different parametrizations of the potential.

TABLES

TABLE I. Parameters in GBD, WPKDG and SHE models.

Model	A [MeV]	B [MeV]	C [MeV]	σ	Λ	$\Lambda_{\rm iso}$	$\Lambda_{\rm aniso}$
GBD	−144.9	203.3	−75.0	7/6	$1.5\,p_F^{(0)}$	—	—
WPKDG	−110.44	140.9	−64.95	1.24	$1.58\,p_F^{(0)}$	—	—
SHE	−110.63	132.17	−53.04	1.27	—	$1.98\,p_F^{(0)}$	$1.41\,p_F^{(0)}$